**Abstract. Yield surface for bending moment, shear force and normal force**

Upper bound limit analysis requires the relationship between interacting forces, termed the yield surface, to be derived on a kinematical basis. A yield surface for bending moment and shear force, which interact in a plastic hinge of a beam, is derived on the basis of the strain rate distribution corresponding to the cross-sectional deformation rates. Beams with a wide and with a square cross-section are treated with the incorporation of Von Mises' distortion energy yield criterion or Tresca's maximum shear stress yield criterion. The kinematically induced yield surface forms a more fundamental alternative to the so-called stress-field induced yield surfaces, as is demonstrated. The theory is extended to include a normal force interacting with bending moment and shear force, for use in generalised yield line theory. This yield surface is applied in an approximate method for predicting the post-buckling collapse load of an in-plane loaded plate.

Keywords: plasticity, limit analysis, upper bound theory, yield line theory, generalised yield line, yield surface.

# Yield surface for bending moment, shear force and normal force

## 1 Introduction

The derivation of a yield surface for bending moment, normal force and in-plane shear force acting along a yield line in a thin plate is part of an investigation into the post-buckling behaviour of such plates (Out, 1982). The post-buckling behaviour was approximated by assuming the material to be rigid plastic and utilising yield line analysis methods.

Classical yield line theory is a limit analysis technique and produces an upper bound for the limit load. Yield line theory is widely used in the analysis of concrete slabs, loaded by forces perpendicular to the plate, since it provides a convenient way of obtaining an insight into the magnitude of the limit load. Upper bound analysis involves choosing a collapse mechanism and calculating the limit load by equating the energy dissipated with the external work performed (Save, 1972).

The buckling behaviour of a plate, however, is a geometrically non-linear phenomenon and therefore limit analysis theorems do not apply. The analysis cannot be proven to produce an upper bound for the collapse load as a function of the displacement of the loaded edge, but it does serve as a tool in an engineering environment. The analysis is "in the spirit" of upper bound limit analysis, i.e., it is based on kinematical considerations.

The collapse mechanism chosen is a yield line mechanism. The plate is thought to consist of rigid sections joined by yield lines where all deformation takes place and the energy is dissipated. The degrees of freedom describing the motions of the mechanism are few, making this concept simple to apply. Yield lines are simplifications of yield zones as they occur in reality. Full modelling of a yield zone could be done by using slip line theory, which implies that the geometry of the zone has to be modelled in detail. A yield line is two- rather than three-dimensional. In other words, it is a local criterion. An error results from this reduction; for example energy dissipated at the boundary of deformed and undeformed sections is neglected (Drucker, 1956). The yield line method is practical because of its simplicity and the error decreases with the plate thickness.

Classical yield line theory incorporates yield lines in which only bending moments are active. The application referred to above, however, requires that the effects of normal and shear forces on the state of yield are also taken into account. The yield lines may be referred to as generalised yield lines.

The derivation of a yield surface for the combination of bending moment, shear and

normal force acting in the generalised yield lines, which gives the constitutive equations, is in itself analogous to the total upper bound analysis and starts with chosing the collapse mechanism; the strain rates forming the basis of the deformation in the yield line. Because the yield surface itself is an "upper bound" yield surface, it cannot be expected that the collapse load, which results from the upper bound analysis, will approach the real collapse load by refining the yield line pattern (Braestrup, 1970).

This paper first discusses some relevant references. In chapter 3, a yield surface is derived for the interaction of bending moment and shear force in the plastic hinge of a beam. This example, simpler than that of the plate problem, is treated for instructive purposes and also because this combination of forces raises the most difficult analytical problems. The yield surface is derived with the incorporation of Von Mises' distortion energy yield criterion, first for a wide beam and then for a beam with a square cross-section. Next, the latter exercise is repeated with Tresca's yield criterion. The chapter is concluded with examples of yield surfaces based upon an assumed stress distribution. It is noted that such a yield surface may have no theoretical basis, i.e., no corresponding strain-rate distribution is possible.

The example of bending moment, normal force and in-plane shear force, active in a thin plate, is dealt with in chapter 4. It is an extension of the earlier work.

Before the concluding remarks, the application of the yield surface in the approximation of the post-buckling behaviour of a plate is briefly outlined.

## 2 Review of relevant references

An early reference in which a kinematically induced yield surface was derived, is by Drucker (1956), who investigated the influence of a shear force on the plastic moment in a plastic hinge of a beam. Drucker describes why a local yield surface is not a strict upper bound yield surface; the present paper refers to these reasons in section 3.1. Drucker used Tresca's maximum shear stress yield criterion. The strain (rate) distribution corresponds to the example of a relatively wide beam. Section 3.3 shows that this assumption is not necessary.

A sound upper bound analysis for the same situation of interacting bending moment and shear force was made by Green (1954). His analysis clearly shows the intricacy of determining this interaction, which he demonstrates by the example of a cantilever beam subjected to a perpendicular force at its end. The precise end condition and the geometry of the beam's cross-section have a profound influence on the yield surface. The yield surface that Green derives, although a sound upper bound, is not convex, which is required of the real yield surface and which would pose computational problems, if applied in a practical case. It is also clear that an exercise such as this is far removed from the application in problems such as the one outlined in the first paragraph of the Introduction.

Possibly, the concept of generalised yield lines first appeared in a paper by Janas and Sawczuk (1966). They investigated the influence of membrane action that develops in a concrete plate when subjected to transverse loading as a result of the restraint offered by

the plate boundaries. The derivation is based on kinematical grounds, but the yield criterion used, termed the maximum normal stress condition of failure, is characterised by a sharp edge at the intersection of the two constituting cones. From kinematical considerations the stress state has to lie on that sharp edge. The energy dissipation rate in the yield line is calculated but no explicit formulation of the yield surface is made.

A kinematical yield surface for use in problems similar to the present one is given by Dean (1975). To the authors opinion, his derivation falls short on some fundamental points. The constitutive relationship used is the Prandtl-Reuss flow rule, which implicitly means that the Von Mises yield criterion is used. Furthermore, he states that a yield surface based on an assumed stress distribution across the cross-section of a yield line is a lower bound yield surface. This is generally false; a point that will be addressed in section 3.4.

The classical work on plasticity by Ilyushin (1956) is unfortunately relatively inaccessible, because there is no English translation and the French edition has long been out of print. The work contains a very general derivation of a yield surface for all six in-plane stress resultants, which act in a thin shell under plane stress conditions. Plane sections are assumed to remain plane, which means that six deformations parameters are sufficient to fully describe the shell's deformation. The yield criterion of Von Mises has been incorporated with its associated flow law. It is a kinematical yield surface and - after some lengthy rearrangements - it can be verified that is does contain the yield surface presented in this paper, if the applicable cross-section deformation parameters are incorporated and the rest eliminated. The approximate Ilyushin yield surface, which is often used because of its simplicity, does differ substantially from the exact one for this specific purpose, and is non-smooth in addition. Furthermore, it does not correspond to any possible strain-rate distribution across the cross-section.

In conclusion, the novelty of the present work lies not in the final result in the first place, but in the clarity of the derivation, in the fact that it has been put into the context of generalised yield line theory and because, in principle, any yield criterion can be implemented.

## 3 Derivation of yield surface for interaction of bending moment and shear force for beam

### 3.0 *General*

As Drucker pointed out, it is impossible to find a unique yield surface for the forces acting in the cross-section of a beam, if it is taken as a two-dimensional entity (Drucker, 1956). The precise kinematical conditions are of influence, such as the type of support and the geometry of the entire beam, and yield depends upon how the load is statically represented. A limitation of the local yield surface is that the compatibility between hinge and environment is violated, while the energy dissipated because of slip between hinge and environment is neglected.

In the present chapter a yield surface for bending moment and shear force acting in the cross-section of a beam will be derived for a number of conditions, following the

kinematical approach of upper bound theory, but with the above limitations. First, in section 3.1, a yield surface is derived under the assumption that the strain rate in the width direction is zero. This example corresponds to a relatively wide beam. If there is no reason to assume that the strain rate in the width direction follows a different pattern than that in the depth direction, as is the case for a beam with a square cross-section, a different yield surface follows as is shown in section 3.2.

The following section 3.3 also considers a square beam but assumes Tresca's yield criterion. Drucker (1956) already treated the example of a wide beam with the same yield criterion. He considered it necessary, however, to assume the strain rate distribution corresponding to this example of a wide beam, but it is shown that the alternative is possible and a square beam can be dealt with.

Often a yield surface is derived by assuming a certain stress distribution over the beam depth, rather than a strain rate distribution. This leads to a mathematically simpler result, but that final yield surface is obviously not an upper bound yield surface. One might argue that if neither approach is strict, one should take the easier way. It is stated in section 3.4, however, that such an assumed stress distribution does not necessarily correspond to a conceivable strain rate distribution and should be rejected on this ground, in favour of the kinematical approach.

## 3.1 *Yield surface for wide beam using Von Mises' yield criterion*

### 3.1.1 Basic assumptions

Consider a plastic hinge in a beam (Fig. 1). The hinge can be represented by a block of material of width $w$, depth $h$ and length $dn$. Length $dn$ approaches zero such that the cross-sectional deformations and forces can be considered to be constant along the length. The forces acting in this block are the bending moment $M_{nn}$ and the shear force $N_{ns}$.

Since the objective is to derive a yield surface for $M_{nn}$ and$N_{ns}$ following upper bound analysis, the derivation should commence with kinematical considerations. We define

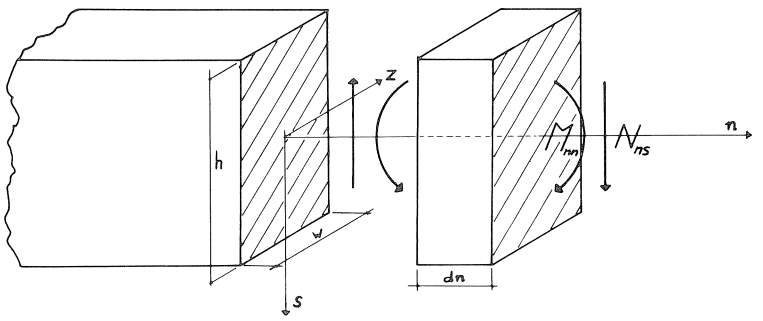


Fig. 1. Plastic hinge with bending moment and shear force.

the deformation rates corresponding to the forces acting in the cross-section:

$$N_{ns} \rightarrow \Delta\dot{u}_s = \dot{\gamma} * dn \tag{3.1.1}$$

$$M_{nn} \rightarrow \Delta\dot{\phi} = \dot{\varkappa} * dn \tag{3.1.2}$$

The outline of the derivation of a yield surface of the forces is as follows. Taking the cross-sectional deformation rates, the next step is to propose a strain rate distribution that is associated with the deformation rates. These kinematical equations are given in section 3.1.2. The strain rates at each point of the cross-section are then translated into a stress distribution by means of the constitutive relationship, as derived in section 3.1.3 for the wide beam. Finally, in section 3.1.4 these constitutive relationships are used to derive the relationship between cross-sectional deformation rates and forces by integration of the stress distribution within the cross-section. Schematically, this means:

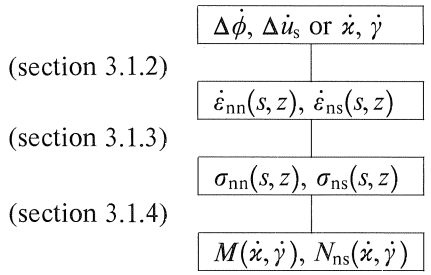


Again, it should be noted that the derivation broadly follows upper bound analysis. The yield surface for $M_{nn}$ and $N_{ns}$, given $\dot{\varkappa}$ and $\dot{\gamma}$, cannot be proved to be an upper bound for the real yield surface, which is specific for each precise statical and kinematical case.

### 3.1.2 Kinematical equations

A simple strain rate distribution, which forms the basis of the rotation and shear deformation rates, is arrived at by assuming:
- shear strain rate and normal strain rate are constant across the width;
- the normal strain rate varies linearly across the depth of the beam, as in simple beam theory;
- the shear strain rate is constant across the depth.

Then, the following strain rate distribution corresponds to the proposed cross-sectional deformation rates:

$$\dot{\varepsilon}_{nn}(s) = \dot{\varkappa} * s \tag{3.1.3}$$

$$\dot{\varepsilon}_{ns}(s) = \dot{\gamma}/2 \tag{3.1.4}$$

The proposed strain rate distribution is the simplest conceivable to produce the required deformation rates; it is also easy to apply, as will be shown in the subsequent

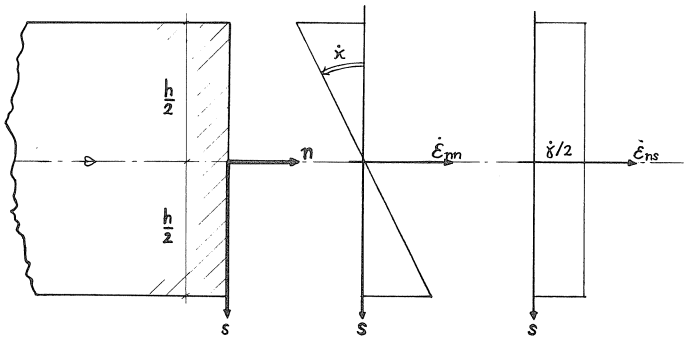


Fig. 2. Strain rate distribution across depth of beam.

sections. It is possible to refine the proposed strain rate distribution in order to lower the upper bound yield surface that will ultimately result from this exercise, for example, by assuming the shear strain rate to vary across the depth. If simplicity is a goal, however, it is useless to attempt to reach perfection by significantly increasing the complexity.

### 3.1.3 Constitutive equations

The constitutive equations, which relate the stress state to the state of the strain rates, are derived in this section.

In general, the strain rate tensor consists of nine components - or six because of symmetry.

$$\dot{\varepsilon}_{ij} = \begin{pmatrix} \dot{\varepsilon}_{nn} & \dot{\varepsilon}_{ns} & \dot{\varepsilon}_{nz} \\ \dot{\varepsilon}_{ns} & \dot{\varepsilon}_{ss} & \dot{\varepsilon}_{sz} \\ \dot{\varepsilon}_{nz} & \dot{\varepsilon}_{sz} & \dot{\varepsilon}_{zz} \end{pmatrix} \tag{3.1.5}$$

For an isotropic material, this can be related to a general stress state by taking a yield criterion and applying the normality rule to find the direction of the strain rate vector. Von Mises' distortion energy criterion is:

$$2\psi = (\sigma_1 - \sigma_2)^2 + (\sigma_2 - \sigma_3)^2 + (\sigma_3 - \sigma_1)^2 \text{ is constant} \tag{3.1.6}$$

After substituting stresses in the $n - s - z$ coordinate system and taking account of the symmetry of the stress tensor, the following holds:

$$\psi = \sigma_{nn}^2 + \sigma_{ss}^2 + \sigma_{zz}^2 - \sigma_{nn}\sigma_{ss} - \sigma_{ss}\sigma_{zz} - \sigma_{zz}\sigma_{nn} + 3\sigma_{ns}^2 + 3\sigma_{sz}^2 + 3\sigma_{zn}^2 - \sigma_M^2 = 0 \tag{3.1.7}$$

where

$\sigma_M$ = the uniaxial yield stress

The normality rule states that:

$$(2 - \delta_{ij})\dot{\varepsilon}_{ij} = \lambda \frac{\partial \psi}{\partial \sigma_{ij}} \qquad i,j = 1,2,3;\ \lambda > 0 \tag{3.1.8}$$

The factor 2, which appears in this equation, stems merely from symmetry: $\dot{\varepsilon}_{ij} = \dot{\varepsilon}_{ji}$; $\delta_{ij}$ is Dirac's function.

The application of this rule to Von Mises' yield criterion gives the following relationship between shear strains and the shear stresses:

$$2\dot{\varepsilon}_{ij} = 6\lambda\sigma_{ij}, \qquad i \neq j \tag{3.1.9}$$

while the subsequent constitutive relationship between normal stresses and strain rates is found:

$$\begin{pmatrix} \dot{\varepsilon}_{nn} \\ \dot{\varepsilon}_{ss} \\ \dot{\varepsilon}_{zz} \end{pmatrix} = \lambda \begin{pmatrix} 2 & -1 & -1 \\ -1 & 2 & -1 \\ -1 & -1 & 2 \end{pmatrix} \begin{pmatrix} \sigma_{nn} \\ \sigma_{ss} \\ \sigma_{zz} \end{pmatrix} \tag{3.1.10}$$

The above matrix is singular and it can be verified that for each stress state the next relationship between the strains holds:

$$\sum_{i=1}^{3} \dot{\varepsilon}_{ii} = 0 \tag{3.1.11}$$

In other words, at yield, the material is incompressible. This result is directly associated with the fact that according to Von Mises an added hydrostatic stress does not produce or influence yield.

In the case under consideration, shear deformation is limited to the $n-s$ plane. Consequently, the shear strain rates $\dot{\varepsilon}_{nz}$ and $\dot{\varepsilon}_{sz}$ must be zero:

$$\dot{\varepsilon}_{nz} = \dot{\varepsilon}_{sz} = 0 \quad \text{and} \quad \dot{\varepsilon}_{ns} \neq 0 \tag{3.1.12}$$

and thus from equation (3.1.9) it is seen that:

$$\sigma_{sz} = \sigma_{nz} = 0 \quad \text{and} \quad 6\lambda\sigma_{ns} = 2\dot{\varepsilon}_{ns} \tag{3.1.13}$$

Now consider the normal strain rates $\dot{\varepsilon}_{ss}$ and $\dot{\varepsilon}_{zz}$. In principle, these are not needed, i.e. they do not correspond to any of the imposed actions. It is not possible, however, to demand that both be zero, since this would violate the requirement of incompressibility, equation (3.1.11).

Thus, since:

$$\dot{\varepsilon}_{nn} + \dot{\varepsilon}_{ss} + \dot{\varepsilon}_{zz} = 0 \tag{3.1.14}$$

then:

$$\dot{\varepsilon}_{ss} + \dot{\varepsilon}_{zz} = -\dot{\varepsilon}_{nn} \tag{3.1.15}$$

Strain rates $\dot{\varepsilon}_{ss}$ and $\dot{\varepsilon}_{zz}$ are thus restricted, but one degree of freedom remains. At the same time $\dot{\varepsilon}_{zz}$ must be bounded by $\dot{\varepsilon}_{nn}$ and $\dot{\varepsilon}_{ss}$ to ensure that the principal strain rates in the $n-s$ plane are the extreme two and that deformation takes place in this plane.

Consider the case of a wide beam, i.e. the depth dimension ($h$) is significantly smaller than the width ($w$). Then, it is reasonable to assume that the strain rate in the width

direction $\dot{\varepsilon}_{zz}$ is negligible:

$$\dot{\varepsilon}_{zz} = 0 \tag{3.1.16}$$

According to equation (3.1.15) it now follows for $\dot{\varepsilon}_{ss}$ that:

$$\dot{\varepsilon}_{ss} = -\dot{\varepsilon}_{nn} \tag{3.1.17}$$

From the set of equations in equation (3.1.10) it can be derived that, given the singular matrix, for the stress state this state of strain rates requires that:

$$-\sigma_{ss} + 2\sigma_{zz} = \sigma_{nn} \tag{3.1.18}$$

The stress state is not a direct function of the strain rate state, but one degree of freedom remains to be chosen on the basis of static considerations. For the wide beam, it is reasonable to assume that the normal stress in the depth direction is negligible:

$$\sigma_{ss} = 0 \tag{3.1.19}$$

From equation (3.1.18) it follows that:

$$\sigma_{zz} = \sigma_{nn}/2 \tag{3.1.20}$$

Substituting equations (3.1.13-19-20) into equation (3.1.7), the Von Mises' yield criterion reduces to:

$$\psi^* = \tfrac{3}{4}\sigma_{nn}^2 + 3\sigma_{ns}^2 - \sigma_M^2 = 0 \tag{3.1.21}$$

leaving $\sigma_{nn}$ and $\sigma_{ns}$ as the only free and independent stress tensor components. The yield criterion is projected onto the $\sigma_{ss} = 0$ plane, rather than intersected with that plane.

The relationship between the independent deformation rates $\dot{\varepsilon}_{nn}$ and $\dot{\varepsilon}_{ns}$ and the corresponding independent stress tensor components can now be established, using equations (3.1.10, 13, 19-20):

$$\begin{pmatrix} \dot{\varepsilon}_{nn} \\ 2\dot{\varepsilon}_{ns} \end{pmatrix} = \lambda \begin{pmatrix} \frac{3}{2}\sigma_{nn} \\ 6\sigma_{ns} \end{pmatrix} = \tfrac{3}{2}\lambda \begin{pmatrix} \sigma_{nn} \\ 4\sigma_{ns} \end{pmatrix}, \qquad \lambda > 0 \tag{3.1.22}$$

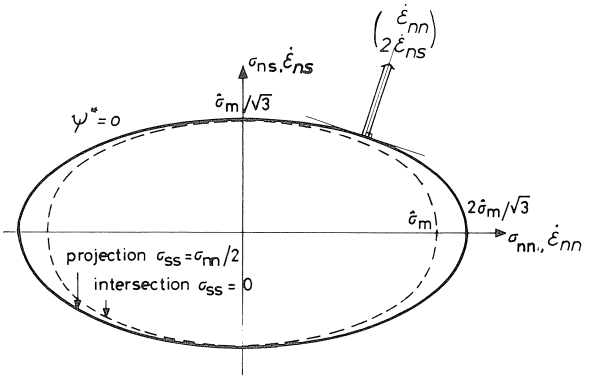


Fig. 3. Reduced Von Mises' yield criterion.

or, the reciprocal relationship:

$$\begin{pmatrix}\sigma_{nn}\\ \sigma_{ns}\end{pmatrix}=\mu\begin{pmatrix}\dot{\varepsilon}_{nn}\\ \dot{\varepsilon}_{ns}/2\end{pmatrix},\qquad \mu>0 \tag{3.1.23}$$

This relationship can also be derived directly from equation (3.1.21) by applying the normality rule.

The stress state must be in a state of yield and must therefore satisfy equation (3.1.21) and this allows, through substitution of equation (3.1.23), elimination of $\mu$ and the unique definition of the stress state as a function of the state of strain rates. Hence it follows that:

$$\sigma_M^{-1}\begin{pmatrix}\sigma_{nn}\\ \sigma_{ns}\end{pmatrix}=\frac{1}{\sqrt{3}}\left[\dot{\varepsilon}_{nn}^2+\dot{\varepsilon}_{ns}^2\right]^{-1/2}\begin{pmatrix}2\dot{\varepsilon}_{nn}\\ \dot{\varepsilon}_{ns}\end{pmatrix} \tag{3.1.24}$$

### 3.1.4 Yield surface for bending moment and shear force

According to the upper bound theorem an upper bound for the limit load is found by equating the virtual change of work performed by the external loads $W$ to the virtual change of the internally dissipated energy $D$. $W$ and $D$ are functions of the independent displacements.

The structure being loaded is the plastic hinge in the beam (Fig. 1) and the acting loads are the bending moment and shear force. The independent displacements corresponding to the loads are rotation and shear deformation of the hinge. As stated above, an upper bound for the yield surface of bending moment and shear force is found by equating $W$ to $D$. Thus:

$$W=D$$

$$M_{nn}\delta\Delta\phi+N_{ns}\delta\Delta u_s=\int_V\sigma_{ij}\delta\varepsilon_{ij}\,dV \tag{3.1.25}$$

By substituting equation (3.1.24) into this expression, while observing that the other stresses do not contribute to the internally dissipated energy, it is found that:

$$M_{nn}\delta\Delta\phi+N_{ns}\delta\Delta u_s=\int_A\left[\sigma_{nn}s\delta\Delta\phi+\sigma_{ns}\delta\Delta u_s\right]dA \tag{3.1.26}$$

or

$$M_{nn}\delta\Delta\phi+N_{ns}\delta\Delta u_s=\left[\int_A\sigma_{nn}s\,dA\right]\delta\Delta\phi+\left[\int_A\sigma_{ns}\,dA\right]\delta\Delta u_s \tag{3.1.27}$$

Displacements $\Delta\phi$ and $\Delta u_s$ are independent and arbitrary. Therefore, the next equalities hold:

$$M_{nn}=\int_A\sigma_{nn}s\,dA \tag{3.1.28}$$

$$N_{ns}=\int_A\sigma_{ns}\,dA \tag{3.1.29}$$

Substitution of equations (3.1.3–4) into equation (3.1.24) produces the stress distribution across the cross-section as a function of the deformation rates:

$$\frac{\sigma_{nn}}{\sigma_M} = \frac{2}{\sqrt{3}} \frac{\dot{\varkappa} s}{\sqrt{(\dot{\varkappa} s)^2 + (\dot{\gamma}/2)^2}} = \frac{2}{\sqrt{3}} \frac{\dot{\varkappa}}{|\dot{\varkappa}|} \frac{s'}{\sqrt{(s')^2 + \omega_s^2}} \tag{3.1.30}$$

$$\frac{\sigma_{ns}}{\sigma_M} = \frac{1}{\sqrt{3}} \frac{\dot{\gamma}/2}{\sqrt{(\dot{\varkappa} s)^2 + (\dot{\gamma}/2)^2}} = \frac{1}{\sqrt{3}} \frac{\dot{\varkappa}}{|\dot{\varkappa}|} \frac{\omega_s}{\sqrt{(s')^2 + \omega_s^2}} \tag{3.1.31}$$

where $s' = 2s/h$

$$\omega_s = \frac{S_p}{2M_p} * \frac{\dot{\gamma}}{\dot{\varkappa}} = \frac{1}{h} \frac{\dot{\gamma}}{\dot{\varkappa}}$$

$$S_p = \frac{\sigma_M}{\sqrt{3}} wh; \qquad \text{the fully plastic shear force}$$

$$M_p = \frac{2\sigma_M}{\sqrt{3}} w(h/2)^2; \qquad \text{the fully plastic bending moment}$$

Integrating equations (3.1.28–29) using the above stress distributions results in:

$$m = \frac{M_{nn}}{M_p} = \frac{\dot{\varkappa}}{|\dot{\varkappa}|} \left[ \sqrt{(1+\omega_s^2)} - \omega_s^2 \ln \frac{1+\sqrt{(1+\omega_s^2)}}{|\omega_s|} \right] \tag{3.1.32}$$

$$s = \frac{N_{ns}}{S_p} = \frac{\dot{\varkappa}}{|\dot{\varkappa}|} \omega_s \ln \frac{1+\sqrt{(1+\omega_s^2)}}{|\omega_s|} \tag{3.1.33}$$

These expressions define a quasi-upper bound yield surface for the interaction of the bending moment and the shear force. It is graphically represented by the curve $k$ in Fig. 4. The physical significance of the parameter $\omega_s$ is indicated.

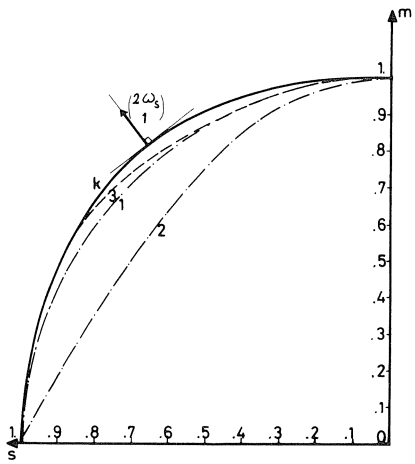


Fig. 4. Yield surfaces for bending moment and shear force.

### 3.2 *Yield surface for square beam using Von Mises' yield criterion*

In this section the yield surface is derived for interacting bending moment and shear force, if the cross-section of the beam is square rather than wide, as was assumed in the previous section. The derivation is analogous to that of the previous section and therefore it is only outlined.

For a square cross-section, the normal shear strain rates in both perpendicular directions (Fig. 1) must be equal.

$$\dot{\varepsilon}_{ss} = \dot{\varepsilon}_{zz} \tag{3.2.1}$$

Incompressibility (equation 3.1.9) requires that:

$$\dot{\varepsilon}_{ss} = -\dot{\varepsilon}_{nn}/2 \tag{3.2.2}$$

According to equation (3.1.10) the stress state must observe the following:

$$\sigma_{ss} = \sigma_{zz} \tag{3.2.3}$$

$$\sigma_{nn} - \sigma_{ss} = \dot{\varepsilon}_{nn}/2\lambda, \qquad \text{with } \lambda > 0 \tag{3.2.4}$$

The latter expression means that, for $\dot{\varepsilon}_{nn} > 0$, $\sigma_{nn} > \sigma_{ss}$. At this point, there is no obvious choice of $\sigma_{ss}$. Like in the previous section, statical considerations must lead to the right choice, see equation (3.1.19), and $\sigma_{ss} = \sigma_{zz}$ can be chosen zero, but in this example this is not so evident, unless the cross-section is small. It will be shown that it is possible to postpone the choice of $\sigma_{ss}$.

The shear strain rate $\dot{\varepsilon}_{ns}$ is related to the shear stress $\sigma_{ns}$ by equation (3.1.13) as before:

$$\sigma_{ns} = \dot{\varepsilon}_{ns}/3\lambda \tag{3.2.5}$$

The yield criterion reduces, given equation (3.2.3), to:

$$\psi^* = (\sigma_{nn} - \sigma_{ss})^2 + 3\sigma_{ns}^2 - \sigma_M^2 = 0 \tag{3.2.6}$$

The stress state is at yield and parameter $\lambda$ can be eliminated by substituting equations (3.2.4) and (3.2.5) into equation (3.2.6):

$$\lambda^{-1} = \frac{2\sigma_M}{\sqrt{\dot{\varepsilon}_{nn}^2 + \frac{4}{3}\dot{\varepsilon}_{ns}^2}} \tag{3.2.7}$$

The bending moment and shear force as a function of the cross-sectional deformation rates are derived directly from the notion that the variation of the energy dissipated in the plastic hinge is equal to the variation of the work performed by the forces bending moment and shear force, as was discussed in section 3.1.4:

The rate of energy dissipated is equal to:

$$\dot{D} = \int_V [\sigma_{nn}\dot{\varepsilon}_{nn} + \sigma_{ss}\dot{\varepsilon}_{ss} + \sigma_{zz}\dot{\varepsilon}_{zz} + 2\sigma_{ns}\dot{\varepsilon}_{ns}]\, dV \tag{3.2.8}$$

$$\dot{D} = (\int_s [(\sigma_{nn} - \sigma_{ss})\dot{\varepsilon}_{nn} + 2\sigma_{ns}\dot{\varepsilon}_{ns}]\, ds) w\, dn \tag{3.2.9}$$

Given equations (3.2.4, 5, 7) this is equal to:

$$\frac{\dot{D}}{w\,\mathrm{d}n} = \sigma_M \int_s \sqrt{[\dot{\varepsilon}_{nn}^2 + \tfrac{4}{3}\dot{\varepsilon}_{ns}^2]}\,\mathrm{d}s \tag{3.2.10}$$

If one then takes the strain rate distribution over the cross-section as before, equations (3.1.3-4), this is equal to:

$$\frac{\dot{D}}{w\,\mathrm{d}n} = \sigma_M \int_{-h/2}^{h/2} \sqrt{[(\dot{\varkappa}s)^2 + \tfrac{4}{3}(\dot{\gamma}/2)^2]}\,\mathrm{d}s \tag{3.2.11}$$

By integration, this is found to be equal to:

$$\frac{\dot{D}}{w\,\mathrm{d}n} = \dot{\varkappa}\sigma_M (h/2)^2 \left[\sqrt{1+\omega_s^2} + \omega_s^2 \ln \frac{1+\sqrt{1+\omega_s^2}}{|\omega_s|}\right] \tag{3.2.12}$$

where

$$\omega_s = \frac{2}{\sqrt{3}h}\frac{\dot{\gamma}}{\dot{\varkappa}} = \frac{S_p}{2M_p}\frac{\dot{\gamma}}{\dot{\varkappa}}$$

The work rate is equal to:

$$\dot{W} = M_{nn}\Delta\dot{\phi} + N_{ns}\Delta\dot{u}_s = M_{nn}\dot{\varkappa}\,\mathrm{d}n + N_{ns}\dot{\gamma}\,\mathrm{d}n \tag{3.2.13}$$

Taking the variations of $\dot{D}$ and $\dot{W}$ with $\dot{\varkappa}$ and $\dot{\gamma}$, we find the following expressions for the bending moment and shear force as a function of the cross-sectional deformation rates:

$$m = \frac{M_{nn}}{M_p} = \frac{\dot{\varkappa}}{|\dot{\varkappa}|}\left[\sqrt{(1+\omega_s^2)} - \omega_s^2 \ln \frac{1+\sqrt{(1+\omega_s^2)}}{|\omega_s|}\right] \tag{3.2.14}$$

$$s = \frac{N_{ns}}{S_p} = \frac{\dot{\varkappa}}{|\dot{\varkappa}|}\,\omega_s \ln \frac{1+\sqrt{(1+\omega_s^2)}}{|\omega_s|} \tag{3.2.15}$$

where

$$M_p = \sigma_M w (h/2)^2$$

$$S_p = \frac{\sigma_M}{\sqrt{3}}\,wh$$

It is concluded that the expressions (3.2.14 and 15) are identical to equations (3.1.32, 33) for the wide beam, except that the fully plastic moment $M_p$ and thus the factor $\omega_s$ are different in both cases: $M_p$ is equal to the fully plastic moment under uniaxial stress, i.e. $\sigma_{ss} = \sigma_{zz} = 0$. The same result could have been arrived at by setting $\sigma_{ss} = 0$ in equation (3.2.4) and integrating stresses as in section 3.1. The condition $\dot{\varepsilon}_{ss} = 0$ for a wide beam is a restraint that raises the yield stress from $\sigma_M$, the uniaxial yield stress, to $(2/\sqrt{3})\sigma_M$. The fully plastic shear force is unaffected, as could be expected. In fact, the choice of $\sigma_{ss} = 0$ has been made implicitly in equation (3.2.13) because any work performed by the stress resultants $M_{ss}$, $M_{zz}$ has been disregarded. This is allowed only if it agrees with statical considerations for the cross-section.

## 3.3 *Yield surface for square beam using Tresca's yield criterion*

### 3.3.1 General

In this section a yield surface for shear force and bending moment will be derived as in the previous section, but this time Tresca's maximum shear stress yield criterion will be incorporated. The strain rate distribution assumed represents the case of a beam with an approximately square cross-section; the strain rates in both lateral directions are assumed to be equal. It is not necessary, as Drucker (1956) stated, to assume that one normal strain rate be zero, forcing the strain rate vector on one of the plane sections of Tresca's hexagonal cylinder. Drucker's assumption implies a beam with a large width-to-depth ratio.

The present assumption means that the strain rate vector is normal to one of the lines of intersection of planes and lies between the two normals to the adjacent planes. It is noted that normality has only limited meaning here.

### 3.3.2 Derivation

Following the reasoning of the previous section, the strain rate tensor is as follows:

$$\dot{\varepsilon}_{ij} = \begin{pmatrix} \dot{\varepsilon}_{nn} & \dot{\varepsilon}_{ns} & 0 \\ \dot{\varepsilon}_{ns} & -\dot{\varepsilon}_{nn}/2 & 0 \\ 0 & 0 & -\dot{\varepsilon}_{nn}/2 \end{pmatrix} \tag{3.3.1}$$

The principal strain rates are:

$$\dot{\varepsilon}_1 = \frac{\dot{\varepsilon}_{nn}}{4} + \frac{\dot{\varepsilon}_{nn}}{|\dot{\varepsilon}_{nn}|}\sqrt{(3\dot{\varepsilon}_{nn}/4)^2 + \dot{\varepsilon}_{ns}^2} \tag{3.3.2}$$

$$\dot{\varepsilon}_2 = -\dot{\varepsilon}_{nn}/2 \tag{3.3.3}$$

$$\dot{\varepsilon}_3 = \frac{\dot{\varepsilon}_{nn}}{4} - \frac{\dot{\varepsilon}_{nn}}{|\dot{\varepsilon}_{nn}|}\sqrt{(3\dot{\varepsilon}_{nn}/4)^2 + \dot{\varepsilon}_{ns}^2} \tag{3.3.4}$$

In the following, it is assumed that $\dot{\varepsilon}_{nn} > 0$, for the tension side of the beam. An analogous conclusion is reached for the compression side, as can easily be demonstrated. Then:

$$\dot{\varepsilon}_3 < \dot{\varepsilon}_2 < \dot{\varepsilon}_1 \tag{3.3.5}$$

From Fig. 5, it is seen that:

$$\tan 2\phi = \frac{\dot{\varepsilon}_{ns}}{3\dot{\varepsilon}_{nn}/4} = \tau \tag{3.3.6}$$

Incompressibility implies that:

$$\frac{\dot{\varepsilon}_1}{\dot{\varepsilon}_2} + \frac{\dot{\varepsilon}_3}{\dot{\varepsilon}_2} + 1 = 0 \tag{3.3.7}$$

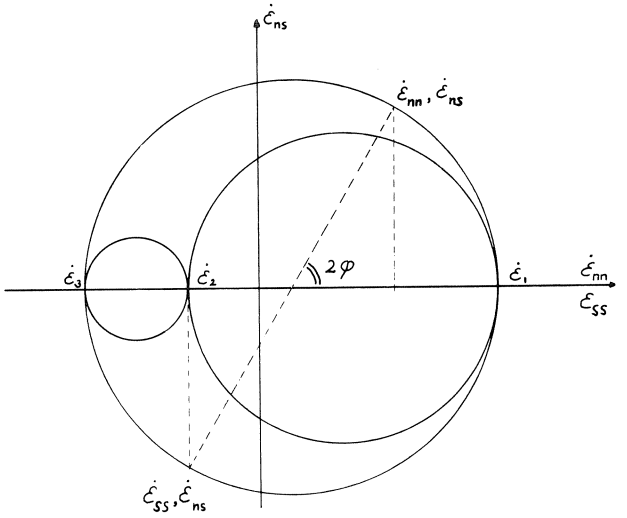


Fig. 5. Circle of Mohr for the state of strain rates.

If $\dot{\varepsilon}_2/\dot{\varepsilon}_3 = \lambda$, with $0 < \lambda < 1$ according to equation (3.3.5), the principal strain rate vector can be written as:

$$\underline{\dot{e}} = \begin{pmatrix} \dot{\varepsilon}_1 \\ \dot{\varepsilon}_2 \\ \dot{\varepsilon}_3 \end{pmatrix} = \eta \left[ \begin{pmatrix} 1 \\ 0 \\ -1 \end{pmatrix} + \lambda \begin{pmatrix} 1 \\ -1 \\ 0 \end{pmatrix} \right] \qquad \text{with } \eta > 0 \tag{3.3.8}$$

In the principal stress space $(\sigma_1, \sigma_2, \sigma_3)$, the vector $(1, 0, -1)$ is the outward normal to the plane:

$$\sigma_1 - \sigma_3 - \sigma_T = 0 \tag{3.3.9}$$

and vector $(1, -1, 0)$ to the plane:

$$\sigma_1 - \sigma_2 - \sigma_T = 0 \tag{3.3.10}$$

These two planes are intersecting planes and it is concluded that the vector $\underline{\dot{e}}$ is normal to the intersection line of the planes and is directed outwards from Tresca's hexagonal cylinder, lying in the fan formed by the normal vectors to the planes (3.3.9-10).

The intersection line is described by the following:

$$\sigma_T^{-1} \underline{\sigma} = \begin{pmatrix} \sigma_1/\sigma_T \\ \sigma_2/\sigma_T \\ \sigma_3/\sigma_T \end{pmatrix} = \begin{pmatrix} 1 \\ 0 \\ 0 \end{pmatrix} + \zeta \begin{pmatrix} 1 \\ 1 \\ 1 \end{pmatrix} \tag{3.3.11}$$

The latter part of this vector represents a hydrostatic stress, which can arbitrarily be added without changing the yield condition. Since the material is incompressible (cf.

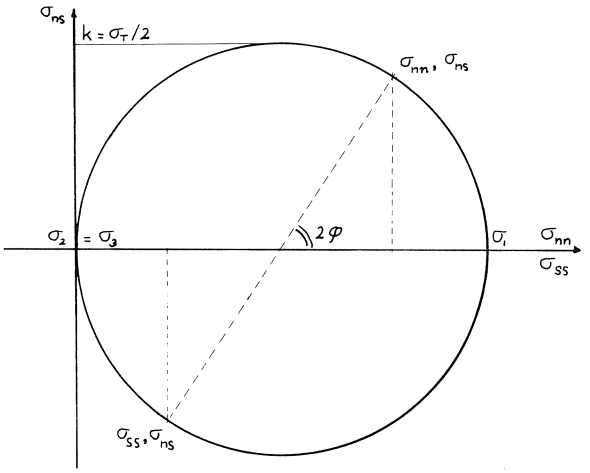


Fig. 6. Circle of Mohr for the stress state.

equation (3.1.11)), it is apparent than this added stress state does not contribute to the rate of dissipated energy and can be disregarded: i.e. $\zeta = 0$.

Mohr's stress circle is shown in Fig. 6. It can be verified that, since $\sigma_{zz} = \sigma_2 = 0$:

$$\tan 2\phi = \frac{2\sigma_{ns}}{\sigma_{nn} - \sigma_{ss}} \tag{3.3.12}$$

Coaxiality of the strain rate tensor and stress tensor means that equation (3.3.12) and equation (3.3.6) must agree. A combination of these equations gives:

$$\sigma_{ns} = \tau(\sigma_{nn} - \sigma_{ss})/2 \tag{3.3.13}$$

Mohr's stress circle (Fig. 6) shows that the following holds, since $\sigma_3 = \sigma_2 = 0$:

$$\sigma_T^2 = (\sigma_{nn} - \sigma_{ss})^2 + 4\sigma_{ns}^2 \tag{3.3.14}$$

where $\sigma_T = 2k$ is the uniaxial yield stress and $k$ is Tresca's yield stress in shear.

From equations (3.3.6, 12-14) the stress state as a function of the strain rate state is:

$$\sigma_{nn}/k = \left[\frac{\dot{\varepsilon}_{nn}}{|\dot{\varepsilon}_{nn}|} + \frac{\dot{\varepsilon}_{nn}}{\sqrt{\dot{\varepsilon}_{nn}^2 + (\frac{4}{3}\dot{\varepsilon}_{ns})^2}}\right] \tag{3.3.15}$$

$$\sigma_{ns}/k = \frac{\frac{4}{3}\dot{\varepsilon}_{ns}}{\sqrt{\dot{\varepsilon}_{nn}^2 + (\frac{4}{3}\dot{\varepsilon}_{ns})^2}} \tag{3.3.16}$$

and also:

$$\sigma_{ss}/k = \left[\frac{\dot{\varepsilon}_{nn}}{|\dot{\varepsilon}_{nn}|} - \frac{\dot{\varepsilon}_{nn}}{\sqrt{\dot{\varepsilon}_{nn}^2 + (\frac{4}{3}\dot{\varepsilon}_{ns})^2}}\right] \tag{3.3.17}$$

We make the same assumption as before for the strain rate distribution:

$$\dot{\varepsilon}_{nn}(s) = \dot{\varkappa} * s \tag{3.3.18}$$

$$\dot{\varepsilon}_{ns}(s) = \dot{\gamma}/2 \tag{3.3.19}$$

Substituting these expressions into equations (3.3.16–17) and integrating across the cross-section results in the following expressions for $M_{nn}$ and $N_{ns}$:

$$m = \frac{M_{nn}}{M_p} = \tfrac{1}{2}\frac{\dot{\varkappa}}{|\dot{\varkappa}|}\left[1 + \sqrt{(1+\omega_s^2)} - \omega_s^2 \ln \frac{1+\sqrt{(1+\omega_s^2)}}{|\omega_s|}\right] \tag{3.3.20}$$

$$s = \frac{N_{ns}}{S_p} = \frac{\dot{\varkappa}}{|\dot{\varkappa}|}\frac{\omega_s}{\sqrt{3}} \ln \frac{1+\sqrt{(1+\omega_s^2)}}{|\omega_s|} \tag{3.3.21}$$

where

$$S_p = kwh = \tfrac{1}{2}\sigma_T wh$$

$$M_p = 2kw\left(\frac{h}{2}\right)^2 = \sigma_T w\left(\frac{h}{2}\right)^2$$

$$\omega_s = \tfrac{2}{3}\frac{S_p}{M_p}\frac{\dot{\gamma}}{\dot{\varkappa}}$$

These expressions hold when $\dot{\varepsilon}_{nn}$ is not equal to 0. When $\dot{\varepsilon}_{nn}$ is equal to 0, it can easily be verified that:

$$\sigma_{nn} = 0$$
$$\sigma_{ns} = k$$
$$N_{ns} = S_p$$
$$M_{nn} = 0$$

In conclusion, the yield surface for a beam with a square cross-section, is discontinuous (Fig. 7). This is a consequence of the piecewise planar shape of Tresca's yield criterion,

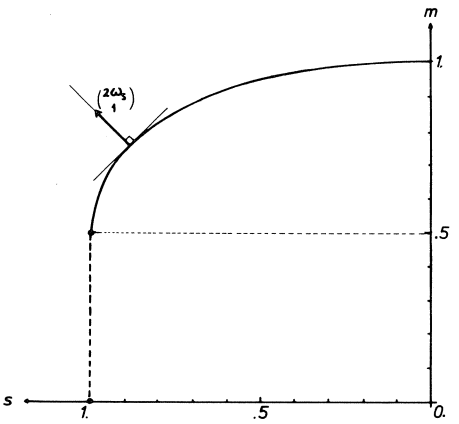


Fig. 7. Yield surface for square beam with Tresca's yield criterion.

to which normality cannot be sensibly applied for all assumed strain rate states. The similarity with yield surface (equations 3.1.32-33), using Von Mises' criterion, is obvious. The yield surface has been "compressed" into the space $0.5 < m < 1$. It is understood why Drucker (1956) considered it necessary to take one of the normal strain rates to be zero, but then the beam with an approximately square cross-section is not covered. This is an effect of the non-smoothness of Tresca's hexagonal cylinder.

## 3.4 *Stress-field induced yield surfaces*

This section briefly touches upon yield surfaces, which are derived by proposing a stress distribution - $\sigma_{nn}(s,z)$, $\sigma_{ns}(s,z)$ - rather than a strain rate distribution over the cross-section of the beam (or analogously, the yield line thickness). For a more complete treatment, the reader is referred to Out, 1981.

A stress-field induced yield surface, in the sense presented in this section, is not a lower bound yield surface, as is sometimes stated. The statical admissibility is not checked. Moreover, some of the yield surfaces derived in this way are not kinematically admissible, which means that no possible strain rate distribution can be found to form

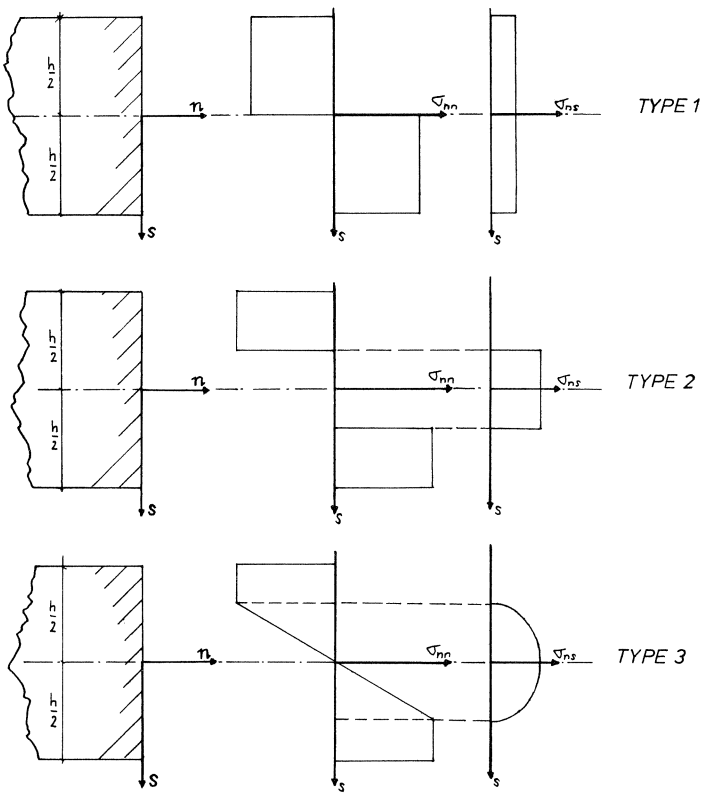


Fig. 8. Assumed stress distributions type 1, 2, 3.

the basis of the respective yield surface. In other cases, the strain rate distribution violates the customary assumption that plane sections remain plane.

The derivation of such a yield surface starts with an assumed stress distribution with some $-n-$ free parameters, which is then integrated across the thickness and width of the beam to produce the yield surface in terms of $n+1$ stress resultants. The stress distribution satisfies the yield criterion, equation (3.1.19) or an alternative yield criterion, since there is no clear basis for this decision. Application of the normality rule on the level of stress resultants then produces the relationship between resultants and cross-sectional deformation rates, rather than strain rates.

Fig. 8 shows three common stress distributions for interaction of shear force and bending moment. Type 2 can easily be verified as having no possible strain rate distribution. Types 1 and 3 violate the requirement of plane sections remain plane, according to the reasoning given in section 3.2 (equation 3.1.22).

The resulting yield surface for bending moment and shear force interaction is shown in Fig. 4. The kinematically induced yield surface, which was derived in section 3.1 is identified by $k$. All three stress-field induced yield surfaces lie below the kinematically induced yield surface, closer when the underlying strain rate distribution is more likely. Both 1 and 2 are non-smooth at $s=1$, considering symmetry about the $s$-axis.

## 4 Yield surface for bending moment, normal force and shear force acting in yield line

### 4.0 *General*

This chapter presents a yield surface for use in generalised yield line theory. The acting forces are bending moment, in-plane shear force and normal force. It applies to plates that are loaded in-plane as well as out-of-plane (cf. e.g. Groeneveld, 1981). The derivation follows upper bound theory, which means that a kinematical concept forms the basis of the analysis, namely the strain rate distribution corresponding to the required yield line deformation rates. This example is analogous to that of the wide beam, treated in section 3.1. Again, the distortion energy yield criterion of Von Mises is assumed, but any yield criterion can be implemented in the procedure.

The derivation is analogous to that given in section 3.1. The addition of the normal force is simply a factor, which adds to the computational complexity. Hence, only an outline of the derivation is given, with differences between the two derivations highlighted.

### 4.1 *Derivation*

The orientation of the yield line is shown in Fig. 9.

The acting forces and the corresponding yield line deformation rates are as follows:

$$N_{nn} \rightarrow \Delta\dot{u}_n = \dot{\bar{\varepsilon}}\, dn$$

$$N_{ns} \rightarrow \Delta\dot{u}_s = \dot{\gamma}\, dn$$

$$M_{nn} \rightarrow \Delta\dot{\phi} = \dot{\varkappa}\, dn$$

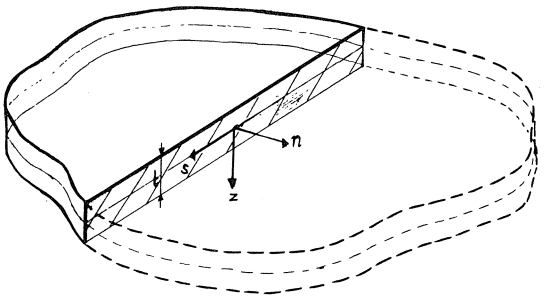


Fig. 9. Orientation of yield line.

The subsequent strain rate distribution is assumed:

$$\dot{\varepsilon}_{nn}(z) = \dot{\bar{\varepsilon}} + \dot{\varkappa} z \tag{4.1.1}$$

$$\dot{\varepsilon}_{ns}(z) = \dot{\gamma}/2 \tag{4.1.2}$$

The following strain rate tensor components are assumed to be zero:
- $\dot{\varepsilon}_{nz}$ and $\dot{\varepsilon}_{sz}$, since shear deformation is limited to the $n-s$ plane;
- $\dot{\varepsilon}_{ss}$, since the length versus width ratio of a yield line is large and the adjacent plate elements rigid; incompressibility then implies that $\dot{\varepsilon}_{zz} = -\dot{\varepsilon}_{nn}$.

For the stress tensor this means:

$$\sigma_{nz} = \sigma_{sz} = 0$$

The following choice for $\sigma_{zz}$ is made:

$$\sigma_{zz} = 0$$

and thus:

$$\sigma_{ss} = \sigma_{nn}/2$$

This is a statical condition, chosen because the plate is assumed to be thin.

Von Mises' yield criterion is reduced to:

$$\psi^* = \tfrac{3}{4}\sigma_{nn}^2 + 3\sigma_{ns}^2 - \sigma_M^2 = 0 \tag{4.1.3}$$

The consequent stress distributions are then:

$$\frac{\sigma_{nn}}{\sigma_M} = \frac{2}{\sqrt{3}} \frac{\dot{\varkappa}}{|\dot{\varkappa}|} \frac{\omega_n + z'}{\sqrt{(\omega_n + z')^2 + \omega_s^2}} \tag{4.1.4}$$

$$\frac{\sigma_{ns}}{\sigma_M} = \frac{1}{\sqrt{3}} \frac{\dot{\varkappa}}{|\dot{\varkappa}|} \frac{\omega_s}{\sqrt{(\omega_n + z')^2 + \omega_s^2}} \tag{4.1.5}$$

with

$$\omega_n = \frac{n_p}{2m_p}\frac{\dot{\bar{\varepsilon}}}{\dot{x}} \quad \text{and} \quad \omega_s = \frac{s_p}{2m_p}\frac{\dot{\gamma}}{\dot{x}}$$

$$z' = 2z/t$$

Integration leads to the yield surface in a parametric representation, graphically represented in Figs. 10-12:

$$\frac{m_{nn}}{m_p} = \frac{\dot{x}}{|\dot{x}|}\,\tfrac{1}{2}\left[a^+b^- - a^-b^+ - \omega_s^2 \ln\left(\frac{a^+ + b^+}{a^- + b^-}\right)\right], \qquad \dot{x} \neq 0$$

$$= 0, \qquad \dot{x} = 0 \qquad (4.1.6)$$

$$\frac{n_{nn}}{n_p} = \frac{\dot{x}}{|\dot{x}|}\,\tfrac{1}{2}[b^+ - b^-], \qquad \dot{x} \neq 0$$

$$= \frac{\dot{\bar{\varepsilon}}}{|\dot{\bar{\varepsilon}}|}\,1/\sqrt{1 + (\omega_s/\omega_n)^2}, \qquad \dot{x} = 0 \qquad (4.1.7)$$

$$\frac{n_{ns}}{n_p} = \frac{\dot{x}}{|\dot{x}|}\,\tfrac{1}{2}\omega_s \ln\left(\frac{a^+ + b^+}{a^- + b^-}\right), \qquad \dot{x} \neq 0$$

$$= \frac{\dot{\gamma}}{|\dot{\gamma}|}\,1/\sqrt{1 + (\omega_n/\omega_s)^2}, \qquad \dot{x} = 0 \qquad (4.1.8)$$

where

$$a^+ = \omega_n + 1$$
$$a^- = \omega_n - 1$$
$$b^+ = \sqrt{(a^+)^2 + \omega_s^2}$$
$$b^- = \sqrt{(a^-)^2 + \omega_s^2}$$

and

$$m_p = \frac{2}{\sqrt{3}}\,\sigma_M (t/2)^2$$

$$n_p = \frac{2}{\sqrt{3}}\,\sigma_M t$$

$$s_p = \frac{1}{\sqrt{3}}\,\sigma_M t$$

The intersections with the planes $m_{nn} = 0$, $n_{nn} = 0$ and $n_{ns} = 0$ are shown in Fig. 10, marked *k*. When $m_{nn} = 0$, it can be verified that:

$$\left(\frac{n_{nn}}{n_p}\right)^2 + \left(\frac{n_{ns}}{s_p}\right)^2 - 1 = 0 \qquad (4.1.9)$$

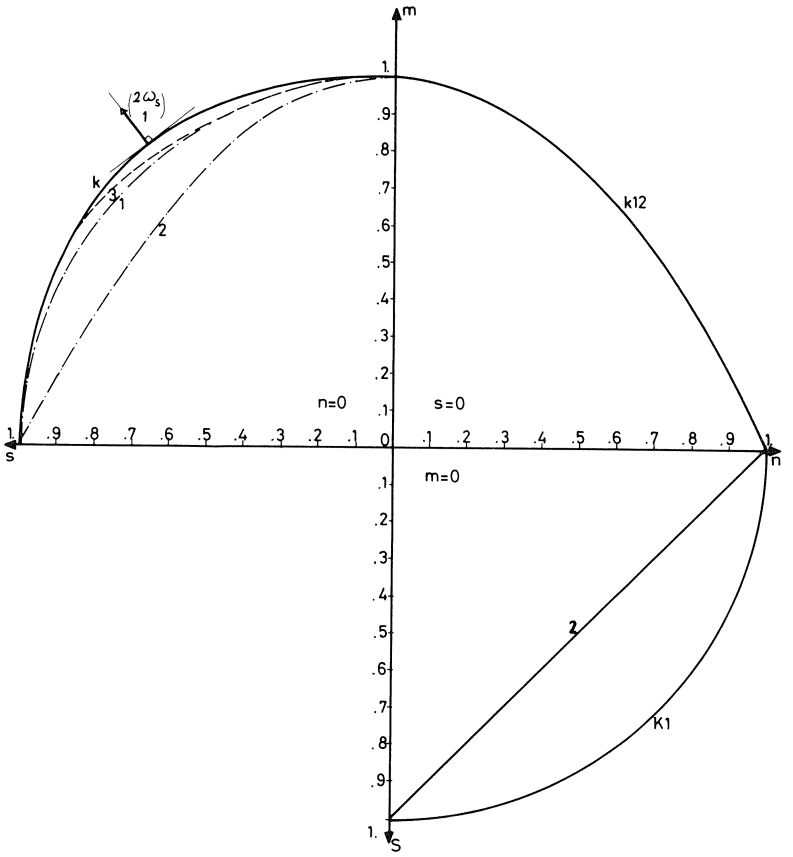


Fig. 10. Intersection of yield surface with planes $m=0$, $n=0$ and $s=0$.

When $n_{ns}=0$, the following holds:

$$\left(\frac{m_{nn}}{m_p}\right)+\left(\frac{n_{nn}}{n_p}\right)^2-1=0 \tag{4.1.10}$$

When $n_{nn}=0$, the yield surface is represented by equations (3.1.32-33).

Figs. 11 and 12 show contour lines of the kinematically induced yield surface as well as the type 1 stress-field induced yield surface (section 3.4.). The physical significance of the $\omega_n$ and $\omega_s$ parameters is indicated. The kinematically induced yield surface lies above or coincides with the type 1 yield surface. In addition, the kinematically induced yield surface is smooth everywhere except for when $n=1$.

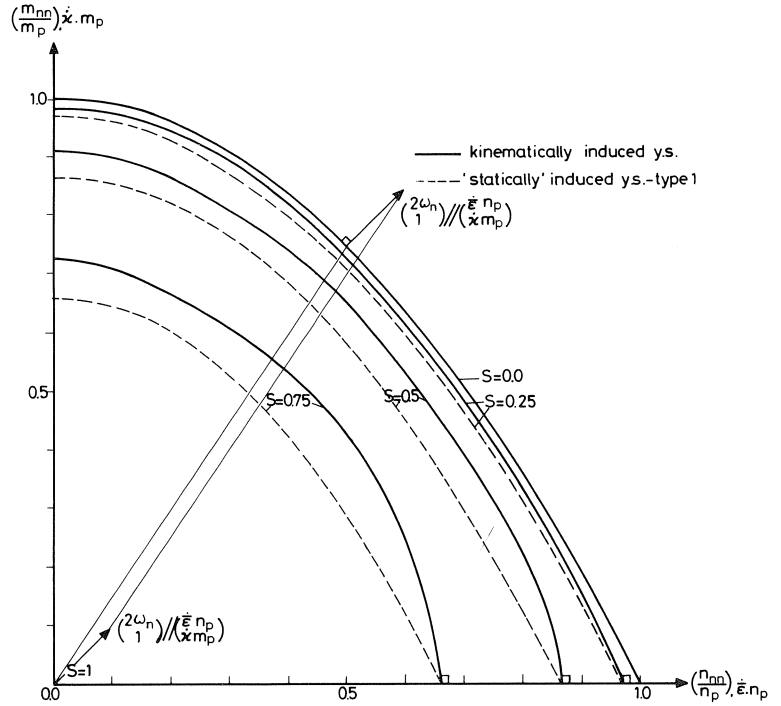


Fig. 11. Contour lines for $s$ in the $m-n$ plane.

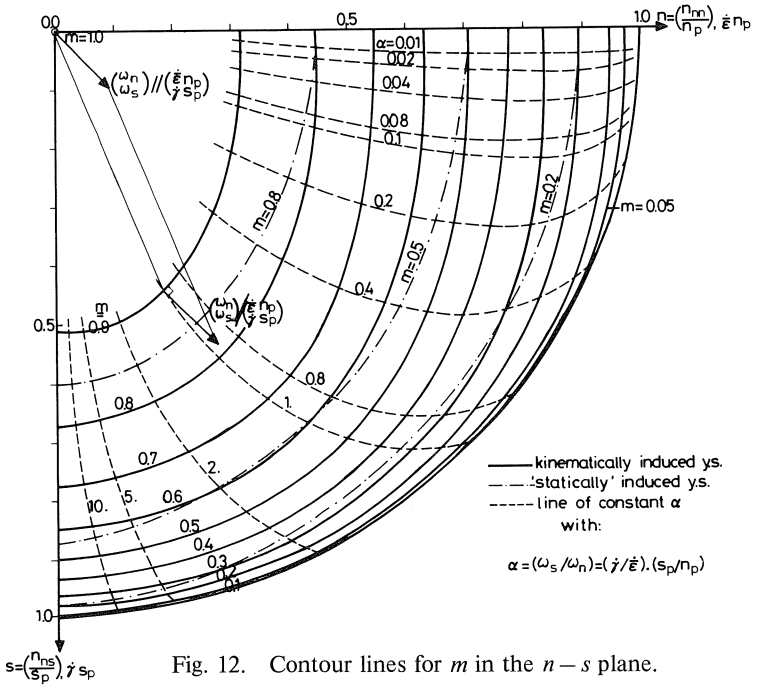


Fig. 12. Contour lines for $m$ in the $n-s$ plane.

## 5 Application: post-buckling behaviour of square plate

### 5.0 *General*

The incentive to develop the yield surface for bending moment, shear force and normal force arose during an investigation into the post-buckling behaviour of a square plate, loaded at one edge by a constant displacement and restrained at the other (Fig. 13) (Out, 1982).

There are sophisticated computer programmes for determining this behaviour, based on the finite element method and incorporating physical and geometrical non-linearities. The purpose of the work was to investigate whether it was possible to approximate the post-buckling behaviour in an analytical way. It was considered interesting to attempt to create an alternative to the intricacy of the finite element programmes, which do not necessarily produce results that can be accepted without question, particularly in the post-collapse domain. It was thought that analytical methods, with explicit assumptions, might form a reasonable reference.

Analyses were made with the finite element programmes CASPA and DIANA (Puthli 1980, 1981). The analytical alternative was formed by a combination of linear-elastic post-buckling theory (Volmir, 1962) and the rigid plastic method, using generalised yield line theory. The latter method required the derivation of the yield surface, which is the subject of this paper.

### 5.1 *Validity*

The results presented are obtained from the analysis of the square plate of Fig. 13, with the width: thickness ratio of 60. This represents an intermediate case between a slender and a stocky plate, for which the collapse load is appreciably higher than the buckling load, and large displacements before the introduction of plasticity are not involved. The

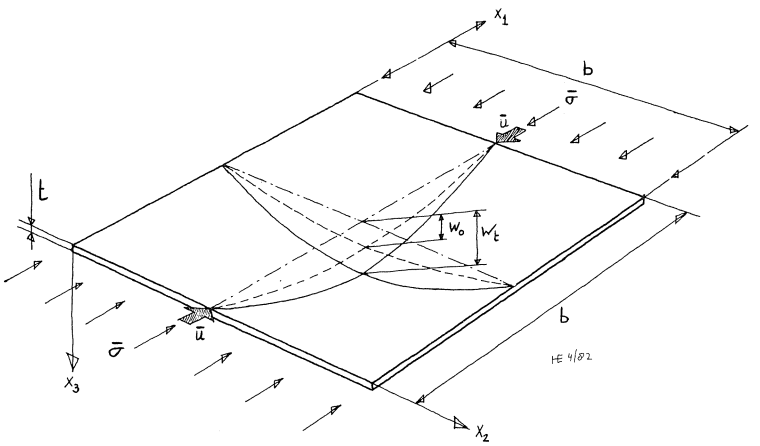


Fig. 13. In-plane loaded square plate.

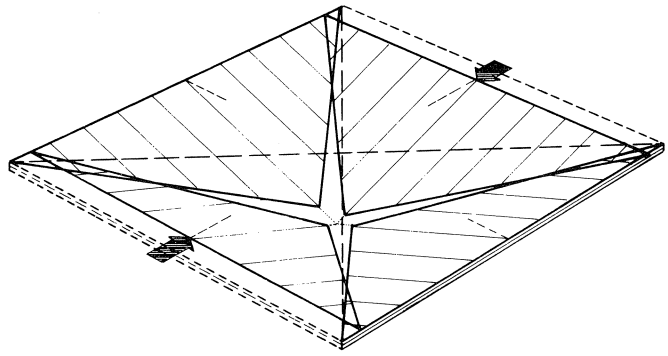

Fig. 14. Cross-shaped yield line mechanism.

yield line mechanism proposed has the simple cross-shape, shown in Fig. 14, which proved to produce the lowest "upper-bound" in the region of interest.

The kinematical equations used were second order polynominal approximations. For this mechanism, the resulting expressions for the yield line deformation rates are:

$$\dot{\bar{\varepsilon}}\, \mathrm{d}n = \Delta \dot{u}_{\mathrm{n}} = \frac{b}{\sqrt{2}} \left[ -\frac{\dot{\bar{u}}}{b} + x' \frac{4\bar{w}\dot{\bar{w}}}{b^2} \right] \tag{5.1.1}$$

$$\dot{\gamma}\, \mathrm{d}n = \Delta \dot{u}_{\mathrm{s}} = \frac{b}{\sqrt{2}} \frac{\dot{\bar{u}}}{b} \tag{5.1.2}$$

$$\dot{\varkappa}\, \mathrm{d}n = \Delta \dot{\phi} = \frac{2\sqrt{2}\dot{\bar{w}}}{b} \tag{5.1.3}$$

where

$x' = \sqrt{2}x/b$ and $x =$ coordinate along the diagonal yield lines, starting at the corner of the plate

The constitutive equations are given by equations (4.1.6–8). With the kinematical equations, they produce the force distributions along the length of the yield line.

The equilibrium equations result from the notion that work rate by the external forces is equal to the rate of energy dissipated in the yield lines. The resulting equations of equilibrium are:

$$\int_0^1 \left[ m_{\mathrm{nn}} + n_{\mathrm{nn}} \frac{\sqrt{2}x\bar{w}}{b} \right] \mathrm{d}x' = 0 \tag{5.1.4}$$

$$\int_0^1 \left[ -n_{\mathrm{nn}} + n_{\mathrm{ns}} \right] \mathrm{d}x' = \frac{F}{b} \tag{5.1.5}$$

The first equation represents the condition that the bending moment around the loaded edge is zero. Equation (5.1.5) represents the balance of the external load with internal forces. Required is force $F$ as a function of $\bar{w}$. The solution strategy involves iteratively

finding the combination of $\dot{\bar{w}}$ and $\dot{\bar{u}}$ as a function of $\bar{w}$, such that equation (5.1.4) is satisfied. Load $F$ then results from equation (5.1.5).

Fig. 15 presents the post-buckling behaviour for this example, in terms of the normalised edge load versus the deflection of the plate. The finite element results for CASPA and DIANA agree very well and are therefore taken as the "real" behaviour. The analytical approximation consists of two components: the linear-elastic curve applies until it meets the rigid-plastic curve, while the point of intersection gives an estimate for the collapse load. At first, the approximation agrees very well, but deviation starts when the plate becomes partially plastic. The collapse load is overestimated by 16% by the analytical method. Part of this can be attributed to the sudden change from linear-elastic to rigid-plastic material behaviour. The "upper bound" rigid plastic collapse behaviour, which incorporates the "upper bound" yield surface, falls above the finite element solutions and follows the shape reasonably well. For increasing deflection, different mechanisms, with a refined yield line pattern, produce lower approximations for the collapse behaviour, though they remain upper bounds (Out, 1982). It is concluded that the analytical method provides an alternative to the purely numerical finite element method, but it must be noted that it cannot be used as a quick and easy reference.

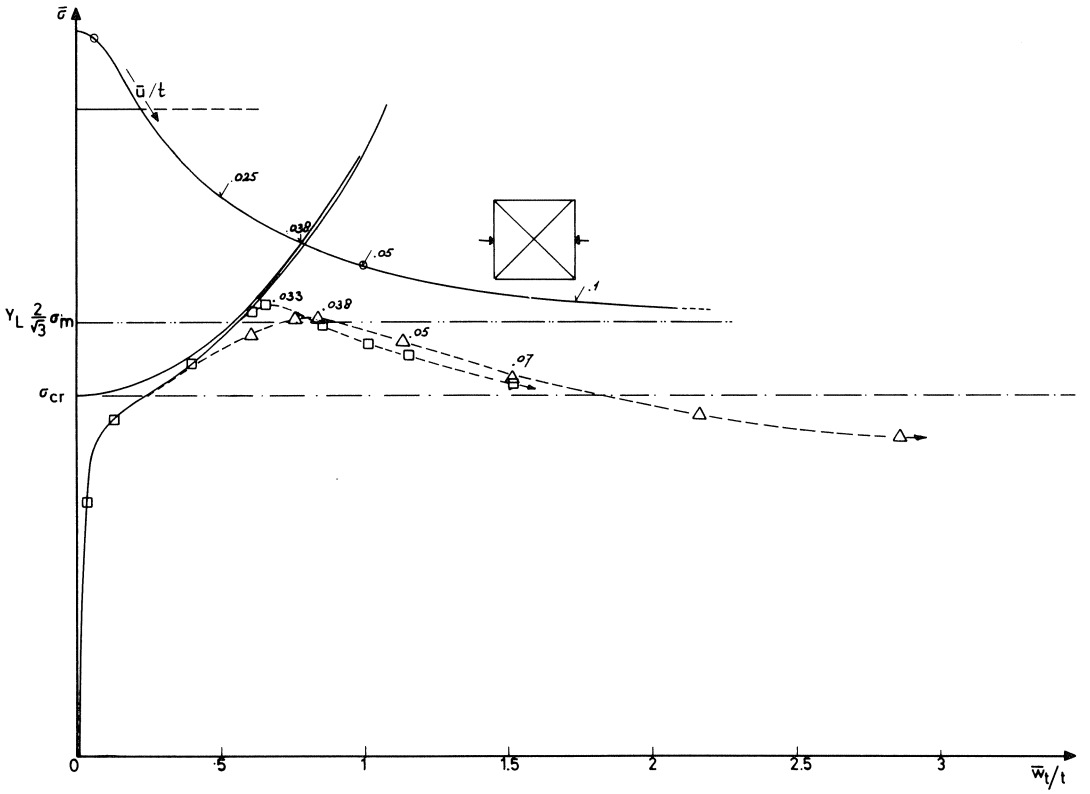


Fig. 15. Post-buckling behaviour of a square plate.

## 6 Summary and conclusions

Local yield surfaces are derived for the interaction of the bending moment and the shear force in a plastic hinge of a beam. The cross-section of the beam is either wide or square. The yield criterion incorporated is either Von Mises' distortion energy yield criterion or Tresca's maximum shear stress yield criterion. The derivation is performed in the context of upper bound limit analysis and is therefore based on kinematical principles. It is concluded that, when Von Mises' yield criterion is applied, the yield surfaces for a wide and for a square cross-section are identical, if normalised with respect to the fully plastic forces. The fully plastic bending moment, however, is influenced by the stress condition invoked by the edge restraint. For the square beam, the stress condition is uniaxial yield; for the wide beam the material yields in plane strain. Both yield surfaces lie above so-called stress-field induced yield surfaces. The incorporation of Tresca's yield criterion poses a problem for the square beam, because it has a piecewise planar shape. The yield surface that is produced is discontinuous.

The yield surface for bending moment, normal force and shear force, which is derived for use in generalised yield line theory, is analogous the yield surface discussed above for a wide beam. Von Mises' yield criterion is implemented. The yield surface is smooth everywhere except at the point where the normal force is fully plastic and lends itself well to the analysis of the post-buckling behaviour of an in-plane loaded plate, as demonstrated in an example. The derivation is quite general and, in principle, any yield criterion can be used instead of Von Mises'.

## 7 Acknowledgements

The work reported in this paper was initiated, while the author worked as a research assistant at IBBC-TNO. The author is indebted to his project supervisors J. Witteveen, F. Bijlaard, C. Hartsuijker and last, not least, A. Vrouwenvelder, for the depth of his knowledge and for reviewing the manuscript. The author would like to thank his present employer, KSEPL, for the permission to publish and for services rendered. J. C. Thieme of PServices provided invaluable assistance.

## 8 Nomenclature

| | |
|---|---|
| $b$ | width of plate |
| $D$ | energy dissipated in a plastically deformed volume |
| $dn$ | length-dimension of plastic hinge |
| $\underline{\dot{e}}$ | vector of principal strain rates |
| $\underline{F}$ | externally applied in-plane load |
| $h$ | depth of beam |
| $k$ | Tresca's yield stress in pure shear |
| $m$ | bending moment, normalised with respect to fully plastic moment |
| $m_{\mathrm{nn}}$ | in-plane bending moment per unit length of yield line |

$m_p$ fully plastic in-plane bending moment per unit length of yield line
$M_{nn}$ bending moment around $z$-axis (beam)
$M_p$ fully plastic bending moment
$n$ - coordinate-axis normal to the plane of plastic hinge or yield line
- normal force, normalised with respect to fully plastic normal force
$n_{nn}$ stress resultant per unit length of yield line in $n$-direction
$n_{ns}$ in-plane shear stress resultant per unit of yield line
$n_p$ fully plastic normal force per unit length of yield line
$N_{nn}$ stress resultant in $n$-direction
$N_{ns}$ shear stress resultant in $s$-direction
$N_p$ fully plastic normal force
$s$ - coordinate-axis in depth direction (beam), along yield line (plate)
- shear force, normalised with respect to fully plastic shear force
$s_p$ fully plastic shear force per unit length of yield line
$S_p$ fully plastic shear force
$t$ plate thickness
$\bar{u}$ in-plane displacement of plate edge with respect to plate centre
$w$ width of beam
$\bar{w}$ deflection of plate centre
$W$ work performed by the external loads
$x$ coordinate along yield line starting at plate corner
$z$ coordinate-axis in width direction (beam), in depth direction (plate)
$\gamma$ engineering shear strain
$\Delta u_n$ deformation in $n$-direction of plastic volume
$\Delta u_s$ shear deformation of plastic volume
$\Delta\phi$ rotation within plastic volume
$\varepsilon_{ij}$ strain tensor components $(i,j = n,s,z)$
$\varepsilon_i$ principal strains $(i = 1,2,3)$
$\varkappa$ bending curvature
$\sigma_{ij}$ stress tensor components $(i,j = n,s,z)$
$\sigma_i$ principal stresses $(i = 1,2,3)$
$\sigma_M$ uniaxial yield stress according to Von Mises
$\sigma_T$ uniaxial yield stress according to Tresca
$\phi$ angle between direction of first principal stress and $n$-direction
$\psi$ plastic potential function
$\omega_n$ normalised extension rate: curvature rate ratio
$\omega_s$ normalised shear rate: curvature rate ratio

## 9 References


BRAESTRUP, M. W. (1970), Yield line theory and limit analysis of plates and slabs, Magazine for Concrete Research, No. 71, Vol. 22, June 1970.

DEAN, J. A. (1975), The collapse behaviour of steel plating subject to complex loading, Ph.D. thesis, Imperial College, London, August 1975.

DRUCKER, D. C. (1956), The effect of shear on the plastic bending of beams, Journal of Applied Mechanics, ASME, December 1956.
GREEN, A. P. (1954), A theory of the plastic yielding due to bending of cantilevers and fixed-end beams, Part 1 & 2, Journal of Mechanics and Physics of Solids, Vol. 3, 1954.
GROENEVELD, H. (1981), Rigid plastic second order calculation of beams and plates, restrained at the edges (in Dutch), TNO-IBBC, Report BI-81-64, 1981.
JANAS, M. and A. SAWCZUK (1966), Influence of the position of lateral restraints on the carrying capabilities of plates, Bulletin d'Information, Comité Européen du Béton, Vol. 58, 1966.
ILYUSHIN, A. A. (1956), Plasticite, Editions Eyrolles, Paris, France, 1956 (out of print).
OUT, J. M. M. (1981), Yield surface for yield line theory based on a kinematical approach, IBBC-TNO, Report BI-82-28, July 1981.
OUT, J. M. M. (1982), The post critical behaviour of a square plate (in Dutch), IBBC-TNO, Report BI-82-27a/c, April 1982.
PUTHLI, R. S. (1980), Collapse analysis of three dimensional assemblages of eccentrically stiffened hot rolled steel plates and shallow shells, HERON, No. 2, Vol. 25, 1980.
PUTHLI, R. S. (1981), Geometrical non-linearity in collapse analysis of thick shells, with application to tubular steel joints, HERON, No. 2, Vol. 26, 1981.
SAVE, M. A. and C. E. MASSONNET (1972), Plastic analysis and design of plates, shells and discs, North Holland Publishing Co., Amsterdam, The Netherlands, 1972.
VOLMIR, A. S. (1962), Biegsame Platen und Schalen, VEB Verlag für Bauwesen, Berlin, DDR, 1962.